Step-wise identification of ultrasound-visible anatomical landmarks for 3D visualization of scoliotic spine

Zachary Baum[1], Ben Church[1], Andras Lasso[1], Tamas Ungi[1,2], Christopher Schlenger[3], Daniel P. Borschneck[2], Parvin Mousavi[4], Gabor Fichtinger[1,2]

1. Laboratory for Percutaneous Surgery, Queen's University, Kingston, Canada
2. Department of Surgery, Queen's University, Kingston, Canada
3. Premier Chiropractic, Stockton, California, USA
4. Medical Informatics Laboratory, Queen's University, Kingston, Canada

ABSTRACT

PURPOSE: Identification of vertebral landmarks with ultrasound is a challenging task. We propose a step-wise computer-guided landmark identification method for developing 3D spine visualizations from tracked ultrasound images.

METHODS: Transverse process bone patches were identified to generate an initial spine segmentation in real-time from live ultrasound images. A modified *k*-means algorithm was adapted to provide an initial estimate of landmark locations from the ultrasound image segmentation. The initial estimations using the modified *k*-means algorithm do not always provide a landmark on every segmented image patch. As such, further processing may improve the result captured from the sequences, owing to the spine's symmetries. Five healthy subjects received thoracolumbar US scans. Their real-time ultrasound image segmentations were used to create 3D visualizations for initial validation of the method.

RESULTS: The resulting visualizations conform to the parasagittal curvature of the ultrasound images. Our processing can correct the initial estimation to reveal the underlying structure and curvature of the spine from each subject. However, the visualizations are typically truncated and suffer from dilation or expansion near their superior and inferior-most points.

CONCLUSION: Our methods encompass a step-wise approach to bridge the gap between ultrasound scans, and 3D visualization of the scoliotic spine, generated using vertebral landmarks. Though a lack of ground-truth imaging prevented complete validation of the workflow, patient-specific deformation is clearly captured in the anterior-posterior curvatures. The frequency of user-interaction required for completing the correction methods presents a challenge in moving towards full automation and requires further attention.

KEYWORDS: Image-Guided Therapy, Spine, Scoliosis, Ultrasound, Visualization, Segmentation, 3D Slicer, SlicerIGT, PLUS Toolkit.

1. PURPOSE

Commonly associated with a coronal curvature in the spine that is greater than 10 degrees, scoliosis is a disease of the spine or spinal deformity and occurs in 1 – 3% of the population [1]. Scoliosis is typically diagnosed in early adolescence and is monitored until the full development of the patient's spine, and beyond [1]. The gold standard for clinical visualization and quantification of scoliosis requires radiographic images to monitor curvature. Monitoring occurs every 4 – 12 months, requiring 10 – 20 radiographs per patient over the course of their adolescence [2]. As regular radiographic monitoring can place patients at a higher risk for cancer [3], infrequent monitoring is common. Additionally, radiographic assessments of the spine are limited to the coronal and sagittal planes which can present clinicians with over-simplified views of the spine [4].

The limitations in visualization and quantification of scoliosis using radiographs motivate using spatially tracked ultrasound as an alternative imaging modality [4, 5]. Ultrasound (US) does not emit ionizing radiation and is portable when compared to radiographic imaging devices. Monitoring and assessing scoliosis, and other spinal deformities, with US has been previously proposed [4, 5]. Spatially tracked ultrasound is capable of precise identification of vertebral landmarks and can provide accurate spinal curvature measurements [5]. This makes it a practical alternative for monitoring and quantifying scoliosis and spinal curvature in patients.

US images can be interpreted for locating landmarks that determine spine orientation [5]. Church *et al.* previously presented qualitatively accurate 3D visualization of scoliotic spines using landmarks acquired from spatially tracked ultrasound images [6]. However, this method requires the user to manually locate each transverse process in US images. Previously, Kamali *et al.* proposed an algorithm for automatic localization of the posterior contours of transverse processes in US

images after the scans had been acquired [7]. Pinter *et al*. presented an adaptation of Kamali *et al.*'s method to localize bone contours in real-time, as the patient is scanned [8].

We propose an approach which helps bridge the gap between segmented bone surfaces and qualitatively accurate 3D visualizations of the spine. By integrating Church *et al.*'s work with that of Pinter *et al.*, our work aims to eliminate the need to review or manually segment patient images through a series of processes to aid in producing 3D visualizations from live US segmentations. We present the methodology and implementation of a computer-aided workflow for landmark identification and generation using US-generated segmented bone surfaces.

2. METHODS

2.1 Initial landmark estimation

A *k*-means algorithm was adapted to provide an initial estimate of landmark locations from the real-time US segmentation (Figure 1). By iterating *k* from 1 to 34 – the number of possible landmarks if each vertebra has two landmarks – the algorithm determines approximate anatomical landmark locations in the segmentation. To prevent unfair preference for larger values of *k*, the error function was multiplied by *k* to serve as a heuristic to allow estimations with less than 34 landmarks. Initial landmark estimations typically produced between 28 and 34 landmarks from a full-length thoracolumbar segmentation (Figure 2). The algorithm was implemented using VTK's (www.vtk.org) *vtkKMeansStatistics* class.

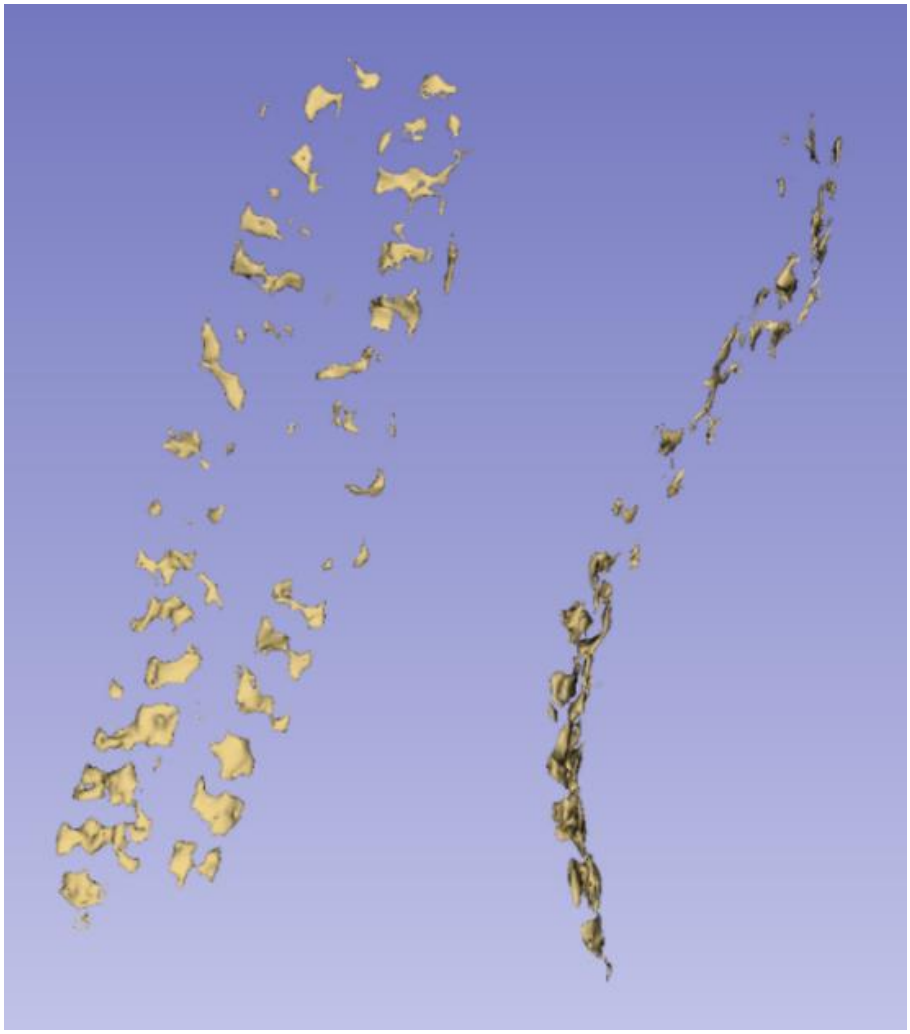

Figure 1: Posterior and left views of results from real-time ultrasound segmentations.

2.2 Landmark set repair

To use Church *et al.*'s 3D spine visualization method, corresponding right and left landmark pairs are required [6]. As shown in Figure 2, the initial estimations using the modified *k*-means algorithm do not always provide a landmark on every segmented patch. There may be multiple points located at a single landmark, landmarks which have no points placed on them, and incorrectly placed points (Figure 2). Further processing may improve the result captured from the segmentation, owing to the spine's symmetries.

2.2.1 Modified k-means clustering:

The bilateral symmetry of the landmarks from the initial estimation renders classification of right and left landmarks possible. Simple *k*-means classification will not be able to classify landmarks as belonging to the right or left side. This is due to the fact that the data may not be linearly separable if the spine is curved. Instead, by sorting the estimated points, we may implement a sliding window *k*-means where only *n* consecutive points are classified in each iteration of the algorithm. As the window slides down, leaving the superior-most point, and incorporating the next inferior-most point, *k*-means is performed again. The window size, n, should be small enough that the points it contains are a short enough segment of the spine so as to be nearly straight, and therefore linearly separable. Too small of a window, however, may result in incorrectly classified points, especially at boundaries with omissions. A window size of 5 landmarks was found to consistently classify left from right sided landmarks for the results presented in this paper. As a single iteration of *k*-means may incorrectly classify a point, the result of each iteration holds one vote in the clustering process for which side the point belongs to.

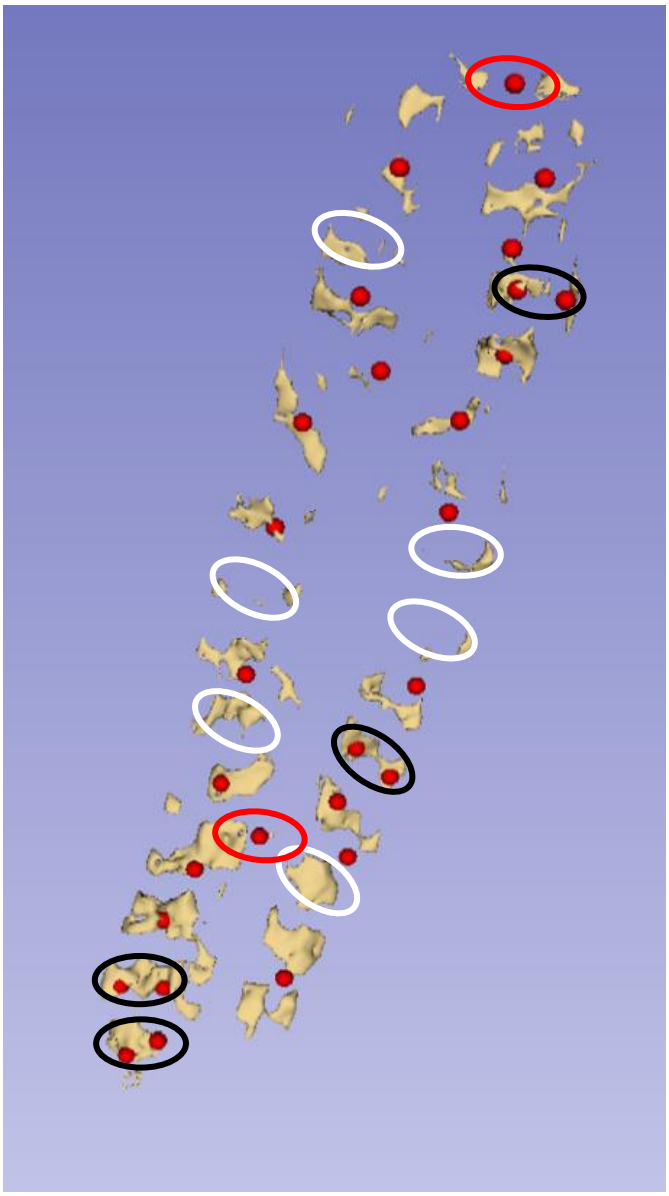

Figure 2: Landmarks defined from initial *k*-means on US segmentation from Figure 1. Duplicates circled in black, missing points circled in white, incorrectly selected points circled in red.

2.2.2 Duplicate landmark removal

Given the axial symmetry of the spine, duplicate points are often characterized by a deviation from normal axial symmetry. Such is to say these duplicates will tend to be 'beside' rather than 'after' one another. To determine if a pair of points was a duplicate, each pair of points was compared to a reference vector. Each reference vector comprised the point immediately preceding and proceeding the possible duplicate pair. Inspecting the angle formed between the potential duplicate vector and the reference vector, it is possible to infer if the pair of points was a duplicate. Duplicate points may be replaced with a new point placed at the average position of the two points.

2.2.3 Missing landmark estimation

Landmarks may be absent from the initial estimation if e.g., there was no segmentation in that region. To impute new points, polynomials were independently fit to the landmarks on the right and left sides. 'Large intervals', or spaces along the fit, may imply missing landmarks. These large intervals were defined as the average interval fit error plus the interval fit error standard deviation. To fill any gaps in these 'large intervals', points were added along the previously acquired polynomial fit. Once an interval is identified as having omitted landmarks, points must be imputed into the interval to

correct the omission. We generate 'patches'; one for each interval with omissions, points are added along the polynomial fit to original points' curve. Points are added to patches based on how much they would improve the interval length polynomial fit if they were included with the rest of the landmarks. Once the change in polynomial fit error corresponding to the inclusion of the new point is no longer large enough, imputation ceases.

2.2.4 Outlier removal

Points deviating medially or laterally from the curvature of other landmarks were considered outliers. Although these points were placed by the initial *k*-means estimation, they may correspond to unintentionally segmented laminae, ribs or anatomical structures. Outliers are detected similarly to duplicates, however instead of observing two points, outlier detection tests individual landmarks in comparison to reference vectors.

2.2.5 User module

A 3D Slicer (www.slicer.org) module was developed to offer several user-configurable options and to allow repairs to the initial *k*-means estimation. Each of the above steps to consolidate, repair and correct points may require quantification and input from the user. Each user-configurable parameter is controlled through the module's user interface.

2.3 Experimental setup and study protocol

Five healthy subjects received thoracolumbar US scans. Subjects had US images taken parasagittally from T1 to L5 while in a natural standing position. This was done to ensure it was possible to acquire up to 34 landmarks – one on either side of the spine for all 17 vertebrae. A SonixTouch US device with a C5-2 transducer (Analogic Corp., Peabody, MA, USA) that is equipped 3D trakSTAR (Northern Digital Inc., Waterloo, ON, Canada) electromagnetic tracker with was used to acquire 2D images from the subjects' spine (Figure 3).

Proper validation of the proposed landmark generation workflow requires imaging for subjects with not only spatially tracked ultrasound taken in the parasagittal orientation, but computerized tomography or radiographic images to obtain ground truth measurements. This combination of data is rare, and performing imaging using ionizing radiation is not justifiable for the sole purpose of validating our methods. Despite the scarcity of available data suitable to fully validate the proposed method, the results and corresponding visualizations for all subjects are given below.

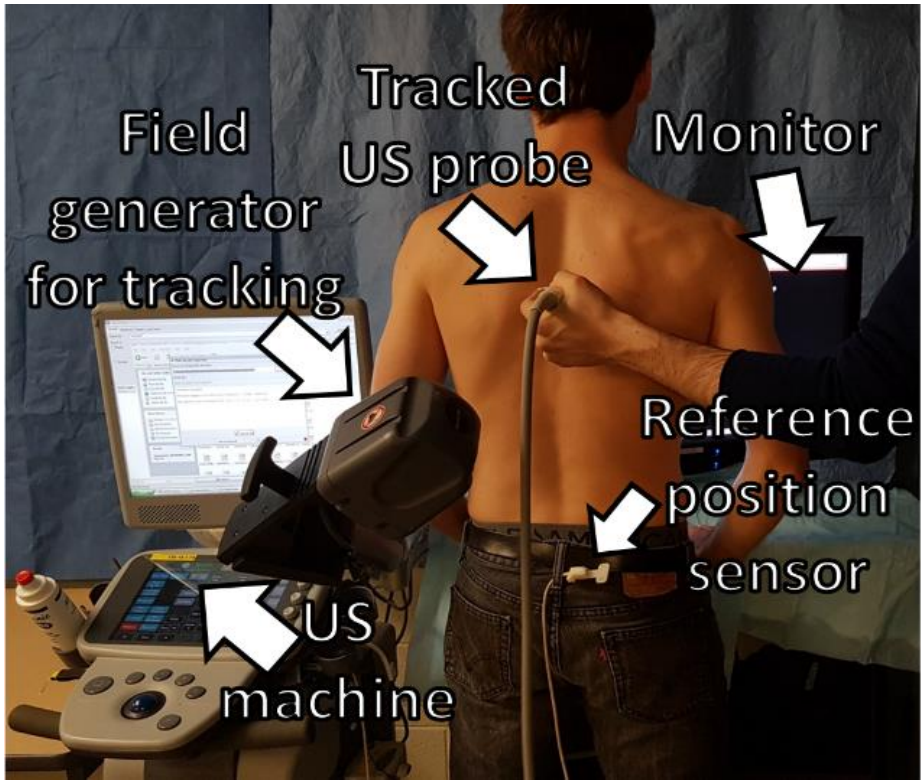

Figure 3: Experimental setup for test data acquisition.

3. RESULTS

Figure 4 shows the major processing steps the data takes; from initial ultrasound segmentation to final surface visualization. Segmentation patches are shown in red, to aid visualization of the sparse data. As mentioned in Section 2.3, no ground-truth data were available for validation. As such, the ultrasound segmentations for all five subjects which were scanned are shown combined with their resulting visualizations in Figure 5.

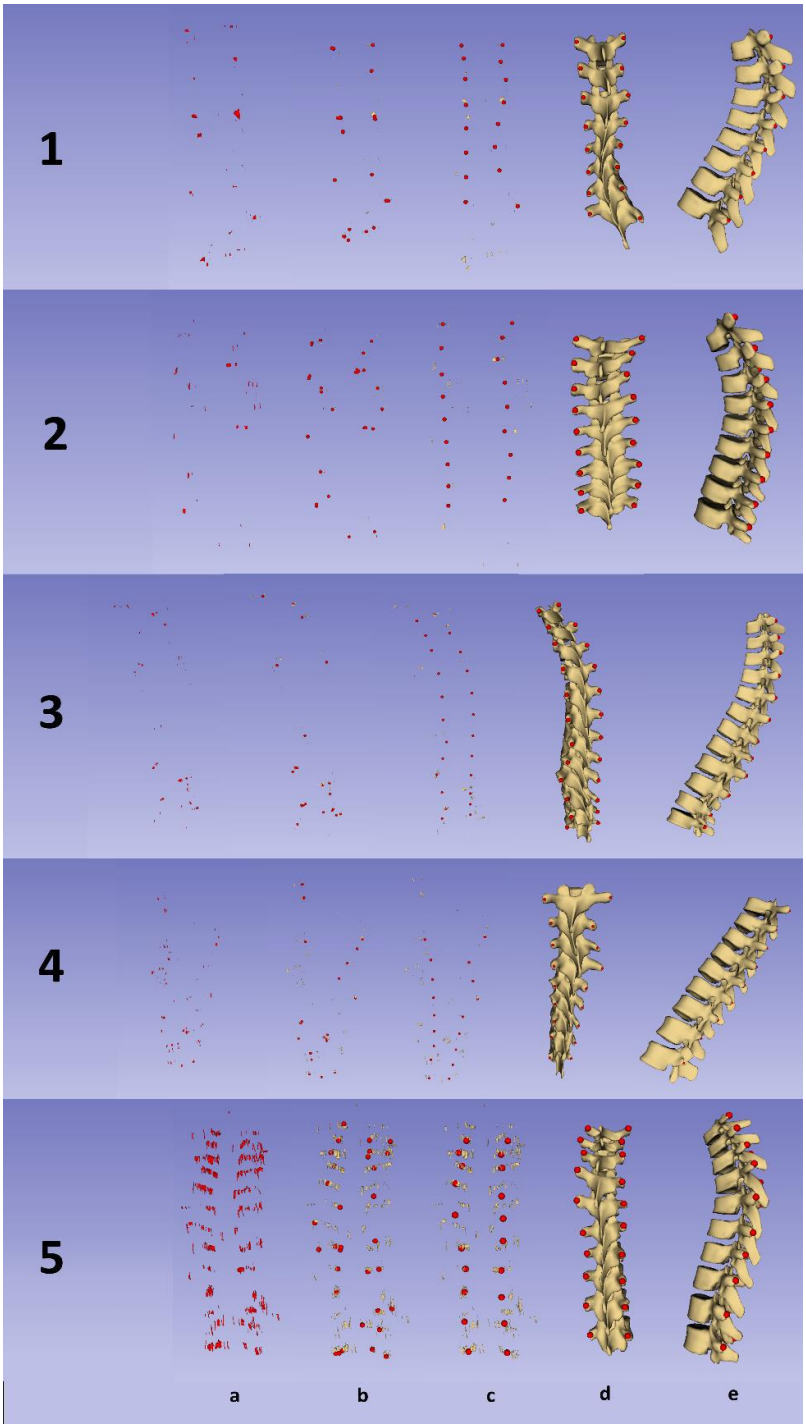

Figure 4: Red segmentation of each subject's ultrasound (a), *k*-means estimate of the landmark locations (red points shown on tan segmentation) (b), landmarks locations after all set repairs are complete (c), posterior view of result (d), left view of result (e)

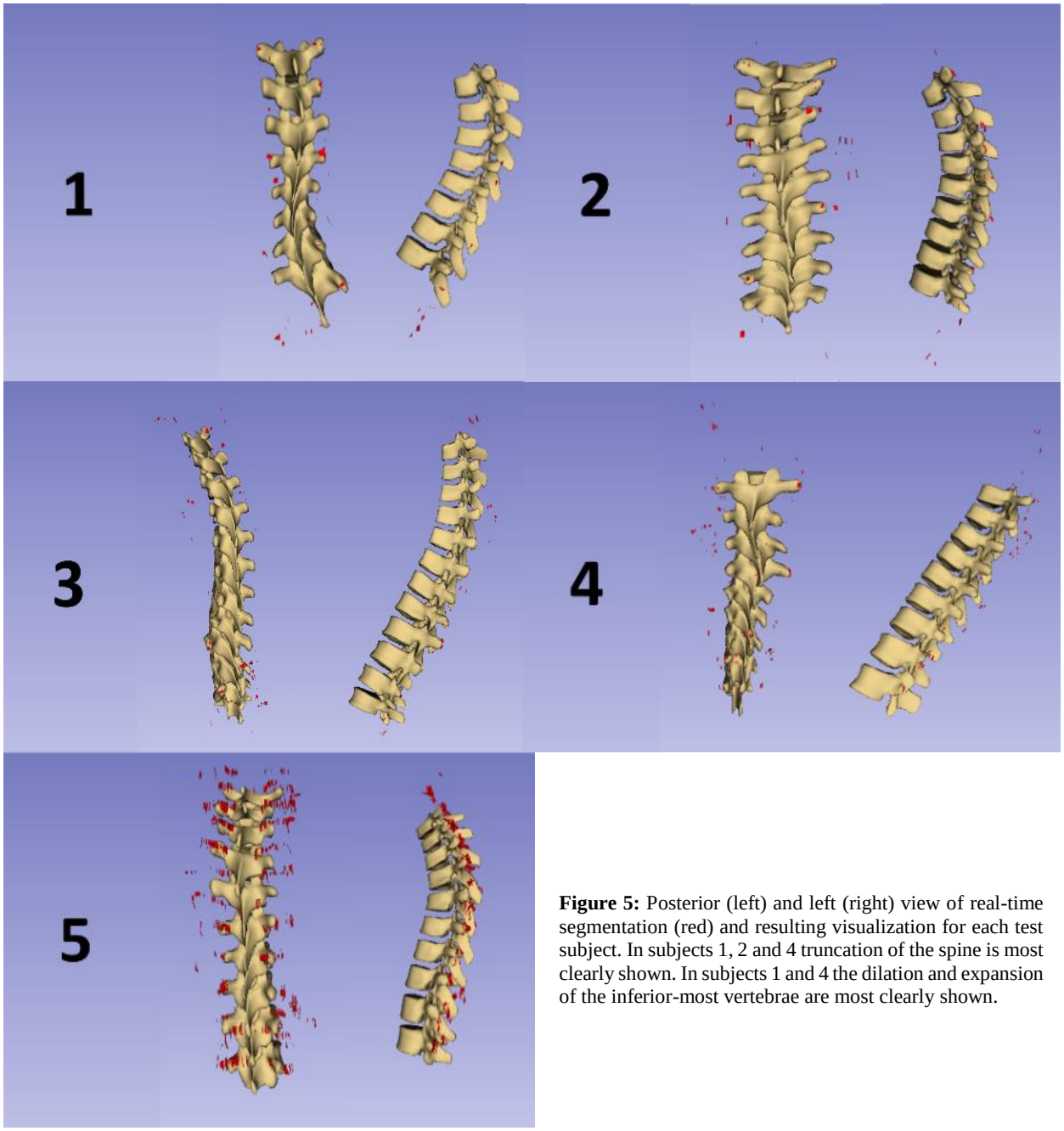

Figure 5: Posterior (left) and left (right) view of real-time segmentation (red) and resulting visualization for each test subject. In subjects 1, 2 and 4 truncation of the spine is most clearly shown. In subjects 1 and 4 the dilation and expansion of the inferior-most vertebrae are most clearly shown.

4. DISCUSSION

The visualizations in Figure 5 can be seen to conform to the parasagittal and anterior-posterior curvatures apparent in the segmentations. The reparation operations described above can correct the initial estimation to reveal the underlying structure and curvature of the spine from each of the subjects. It is qualitatively apparent that these visualizations are not the same quality as those presented by Church *et al.* as the spine is typically truncated and tends to suffer dilation or expansion near the superior and inferior-most points on the visualization. We believe this is larger due to the early stage nature of the real-time segmentation algorithm presented by Pinter *et al.* In this algorithm, the search for ideal segmentation parameters is ongoing and the resulting segmentations are sparser than desired. This sparsity renders the initial estimates inaccurate as the transverse processes may not have been segmented in full.

The segmentations contain several types of defects for which reparations have been designed, but they also contain others. One of the most salient issues in the visualizations is from omitted landmarks at the ends of the spine. Using only the repairs described above, these omissions cannot be corrected. If either side of the spine lacks the superior-most or inferior-most landmarks, the corresponding landmarks on the other side must be discarded. This is due to the pair-wise correspondence that is required for generating visualizations using the landmark registration-based method to generate a thin-plate spline to warp a generic spine model into the subject's anatomy [6]. However, there is other work which adapts the thin-plate spine landmark registration method and does not require pair-wise correspondences for the landmarks [9]. In this approach, by creating an initial registration using the spine's centerline, the registration is updated with every point that is added improving the accuracy and visualization-based estimate [9]. Adapting our proposed method to use a similar initial registration to Baum *et al.*'s may help reduce the risk of losing un-paired landmarks and ensure that the registration does not encounter large truncations.

The intended purpose of the landmark generation aid was to reduce user interaction when compared to manually locating landmarks in a series of ultrasound snapshots. It proved difficult to choose parameters for certain aspects of the repairs such as outlier detection as it is not often clear which points are outliers. During the analysis of the US images, it was found that the user may even wish to delete a point which the initial estimation had placed on a landmark if it was inaccurate enough. This would be done with the intent of re-estimating it with the polynomial fit to provide a new location for the landmark. These errors, among others, present challenges to overcome when minimizing user interaction, as more than one iteration of each repair was often required when analyzing each of the five subjects.

5. CONCLUSION

Our methods encompass a series of steps to bridge the gap between US scans, real-time segmentations of the scans and the 3D spine visualizations that are possible using a pairwise landmark registration method. Our method was used to generate visualizations for five healthy volunteers as test cases. Justifiably, a lack of computerized tomography or radiographic ground-truth prevented rigorous validation of the complete workflow. However, when comparing visualizations with the segmentations, patient-specific deformation is clearly captured in the anterior-posterior curvatures. The modular structure of the landmark generation aid will allow for simple substitution of other segmentation methods. However, the frequency of user-interaction required for completing the correction methods presents a challenge to overcome before full automation is possible.

ACKNOWLEDGEMENTS

Zachary M. C. Baum was supported by the Alexander Graham Bell Canada Graduate Scholarship from the Natural Sciences and Engineering Research Council of Canada (NSERC). Gabor Fichtinger is supported as a Cancer Care Ontario Research Chair in Cancer Imaging. Financial support was received from the SEAMO Educational Innovation and Research Fund. This work was financially supported as a Collaborative Health Research Project (CHRP #127797), a joint initiative between the Natural Sciences and Engineering Research Council of Canada (NSERC) and the Canadian Institutes of Health Research (CIHR).

REFERENCES

[1] L. Goldman and A. I. Schafer, Goldman's Cecil medicine, Philadelphia: Elsevier Saunders, 2012.

[2] M. Doody, M. M. S., J. E. Lonstein, M. Stovall, D. G. Hacker, N. Luckyanov and C. E. Land, "Breast cancer mortality after diagnostic radiography: findings from the U.S. scoliosis cohort study," *Spine*, vol. 25, no. 16, pp. 2052-2063, 2000.

[3] I. Schmitz-Feuerhake and S. Pflugbeil, "'Lifestyle' and cancer rates in former East and West Germany: the possible contribution of diagnostic radiation exposures," *Radiation Protection Dosimetry*, vol. 147, no. 1, pp. 310-313, 2011.

[4] Q. Wang, M. Li, E. H. M. Lou and M. S. Wong, "Reliability and validity study of clinical ultrasound imaging on lateral curvature of adolescent idopathic scoliosis," *PLoS ONE*, vol. 10, no. 8, p. e0135264, 2015.

[5] T. Ungi, F. King, M. Kempston, Z. Keri, A. Lasso, P. Mousavi, J. Rudan, D. P. Borshneck and G. Fichtinger, "Spinal curvature measurement by tracked ultrasound snapshots," *Ultrasound in Medicine & Biology*, vol. 40, no. 2, pp. 447-454, 2014.

[6] B. Church, A. Lasso, C. Schlenger, D. P. Borshneck, P. Mousavi, G. Fichtinger and T. Ungi, "Visualization of scoliotic spine using ultrasound-accessible skeletal landmarks," in *SPIE Medical Imaging*, Orlando, 2017.

[7] S. Kamali, T. Ungi, A. Lasso, C. Yan, M. Lougheed and G. Fichtinger, "Localization of the transverse processes in ultrasound for spinal curvature measurement," in *SPIE Medical Imaging*, Orlando, 2017.

[8] C. Pinter, B. Travers, Z. Baum, S. Kamali, T. Ungi, A. Lasso, B. Church and G. Fichtinger, "Real-time transverse process detection in ultrasound," in *SPIE Medical Imaging*, Houston, 2018.

[9] Z. Baum, T. Ungi, A. Lasso, B. Church, C. Schlenger and G. Fichtinger, "Visual aid for identifying vertebral landmarks in ultrasound," in *SPIE Medical Imaging*, Houston, 2018.